Water Research 254 (2024) 121427

Contents lists available at ScienceDirect

Water Research

journal homepage: www.elsevier.com/locate/watres

The composition and differences of antimony isotopic in sediments affected by the world's largest antimony deposit zone

Huiji Liu [a], Guangyi Sun [b], Mengchang He [a,*], Xinbin Feng [b], Chunye Lin [a], Wei Ouyang [a,c], Xitao Liu [a]

[a] State Key Laboratory of Water Environment Simulation, School of Environment, Beijing Normal University, Beijing 100875, China
[b] State Key Laboratory of Environmental Geochemistry, Institute of Geochemistry, Chinese Academy of Sciences, Guiyang 550081, China
[c] Advanced Interdisciplinary Institute of Environment and Ecology, Beijing Normal University, Zhuhai 519087, China

ARTICLE INFO

Keywords:
Antimony isotopes
Zijiang river
Sediments
Source
Geochemical process

ABSTRACT

Antimony (Sb) isotopic fingerprinting is a novel technique for stable metal isotope analysis, but the use of this technique is still limited, especially in sediments. In this study, the world's most important Sb mineralization belt (the Xikuangshan mineralization belt) was taken as the research object and the Sb isotopic composition and Sb enrichment characteristics in the sediments of water systems from different Sb mining areas located in the Zijiang River (ZR) Basin were systematically studied. The results showed that the ε^{123}Sb values in the sediments of the ZR and its tributaries, such as those near the Longshan Sb-Au mine, the Xikuangshan Sb mine, and the Zhazixi Sb mine, were 0.50−3.13 ε, 2.31−3.99 ε, 3.12−5.63 ε and 1.14−2.91 ε, respectively, and there were obvious changes in Sb isotopic composition. Antimony was mainly enriched in the sediments due to anthropogenic sources. Dilution of Sb along the river and adsorption of Sb to Al-Fe oxides in the sediment did not lead to obvious Sb isotopic fractionation in the sediment, indicating that the Sb isotopic signature was conserved during transport along the river. The Sb isotopic signatures measured in mine-affected streams may have differed from those in the original Sb ore, and further investigation of Sb isotopic fingerprints from other possible sources and unknown geochemical processes is needed. This study reveals that the apparent differences in ε^{123}Sb values across regions make Sb isotopic analysis a potentially suitable tool for tracing Sb sources and biogeochemical processes in the environment.

1. Introduction

Antimony (Sb) pollution is a global problem, and its geochemistry, migration and transport have attracted increasing attention worldwide (Herath et al., 2017). Human activities have caused important changes in Sb cycling on the surface of the earth, and its anthropogenic flux has greatly exceeded its natural flux, accounting for ~83 % of the total flux, with mining being the main factor (~93 %) among anthropogenic sources (Sen and Peucker-Ehrenbrink, 2012). Antimony is not only heavily enriched in rivers, atmospheric aerosols and soils but also exists in peat and ice cores from the Canadian Arctic (Krachler et al., 2005). Antimony enters freshwater systems through rock weathering and leaching, and it can reach values of hundreds or even thousands of μg/L in polluted rivers near mining areas and smelters (He et al., 2012, 2019). The impact of Sb pollution on freshwater systems closely associated with human activities has been of particular concern to researchers. Therefore, it is important to fully understand the origin and behavior of antimony using robust methodologies and direct evidence (i.e., Sb isotopes) to predict its potential mobility, bioavailability and environmental impact in aquatic environments and to initiate associated remediation efforts in mining-affected hydrological systems.

There are two stable isotopes of Sb, ^{121}Sb and ^{123}Sb, which have large masses and a relatively small fractionation range, and their relative abundances are 57.21 % and 42.79 %, respectively (Hoefs, 2018). The high-precision measurement of Sb isotopes has been realized by Multicollector-Inductively Coupled Plasma-Mass Spectrometry (MC-ICP-MS) (Rouxel et al., 2003; Tanimizu et al., 2011; Wen et al., 2018; Liu et al., 2020). Through the study of Sb isotopic composition in different environmental samples, such as water and deep-sea hydrothermal sulfides, it was found that the degree of Sb isotopic composition changes depends on the type of samples analyzed, among which the Sb isotope changes most in hydrothermal sulfides, with a ε^{123}Sb value of

---

* Corresponding author.
E-mail address: hemc@bnu.edu.cn (M. He).

https://doi.org/10.1016/j.watres.2024.121427
Received 3 October 2023; Received in revised form 3 March 2024; Accepted 4 March 2024
Available online 5 March 2024
0043-1354/© 2024 Elsevier Ltd. All rights reserved.

16.9 ε (Rouxel et al., 2003). Researchers have proposed multiple mechanisms to explain Sb isotope fractionation, such as redox transformations (Rouxel et al., 2003; Dillis et al., 2019; Wang et al., 2021) and adsorption to iron (hydr)oxides (Araki et al., 2009; Tanimizu et al., 2011; Zhou et al., 2023). In addition, biomethylation processes lead to heavy isotope enrichment (Wehmeier et al., 2003). These studies demonstrate that Sb isotopes are powerful tools for tracing Sb pollution sources and biogeochemical processes, but the composition and fractionation mechanisms of Sb isotopes in environmental systems still need to be further elucidated. Due to heterogeneity in the biogeochemical characteristics of different mining areas, Sb isotopic composition may change during the process of transmission from mine tributaries to rivers and lakes (Resongles et al., 2015). A study of the isotopic composition of Sb in France revealed that there were differences in the isotopic composition of Sb in two watersheds affected by mining, and the ε^{123}Sb values in the Orb River and Gardon River were −0.6−+1.1 ε and +2.7−+8.3 ε, respectively (Resongles et al., 2015). Currently, the systematic research on the isotopic composition of Sb in aquatic environments is only preliminary reported in river water (Resongles et al., 2015; Wen et al., 2023), and the isotopic composition of Sb in sediments has not been studied. Compared to the water phase, Sb is more inclined to combine with sediments (Liu et al., 2023), and sediments are important hosts for geological records and anthropogenic Sb emissions. However, the impact of complex environmental conditions on the isotopic composition of Sb in sediments is still poorly understood. Therefore, accurately determining the isotopic composition of Sb in sediments is essential for revealing the geological origin of Sb and its source tracing, which is of great significance.

The Zijiang River (referred to as "ZR") is an important tributary of the Dongting Lake Basin in the midstream region of the Yangtze River. The ZR Basin is located in the ultra-large Sb ore belt, and various Sb ores have been confirmed in the basin, for example, the world's largest Sb mine, Xikuangshan, is in this region (Liu et al., 2023). Due to hundreds of years of mining activities, Sb pollution in Xikuangshan is serious, and previous studies have mainly focused on the distribution and speciation of Sb in rivers, groundwater, mine drainage, sediments, soil and mine tailings, and fish (Wang et al., 2011). In addition, Wen et al. (2016, 2022, 2023) used S, Sr, Mo, and Sb isotopic methods to explore the geochemical processes of Sb in water systems and found that Sr, S and Sb have common pollution sources, and the attenuation of Sb in groundwater or mine water is affected by Sb adsorption and desorption to Fe/Mn-(hydr)oxides. However, the development of other Sb mines in the ZR Basin has also increased, and the sources and geochemical processes of Sb in the water system of the ZR affected by these mines are still unclear, especially in the sediments. Therefore, it is important to use advanced methods and means to determine the factors controlling the sources and migration of Sb in the sediment system of the ZR.

The purpose of this study is to analyze Sb isotopic composition characteristics and Sb enrichment and sources in hydrologic sediments affected by different mining areas in the ZR Basin and to elucidate the geochemical processes that affect the source and migration of Sb in the water system. This study supplements the Sb isotope fingerprint database and provides basic data for tracing the source of environmental Sb pollution.

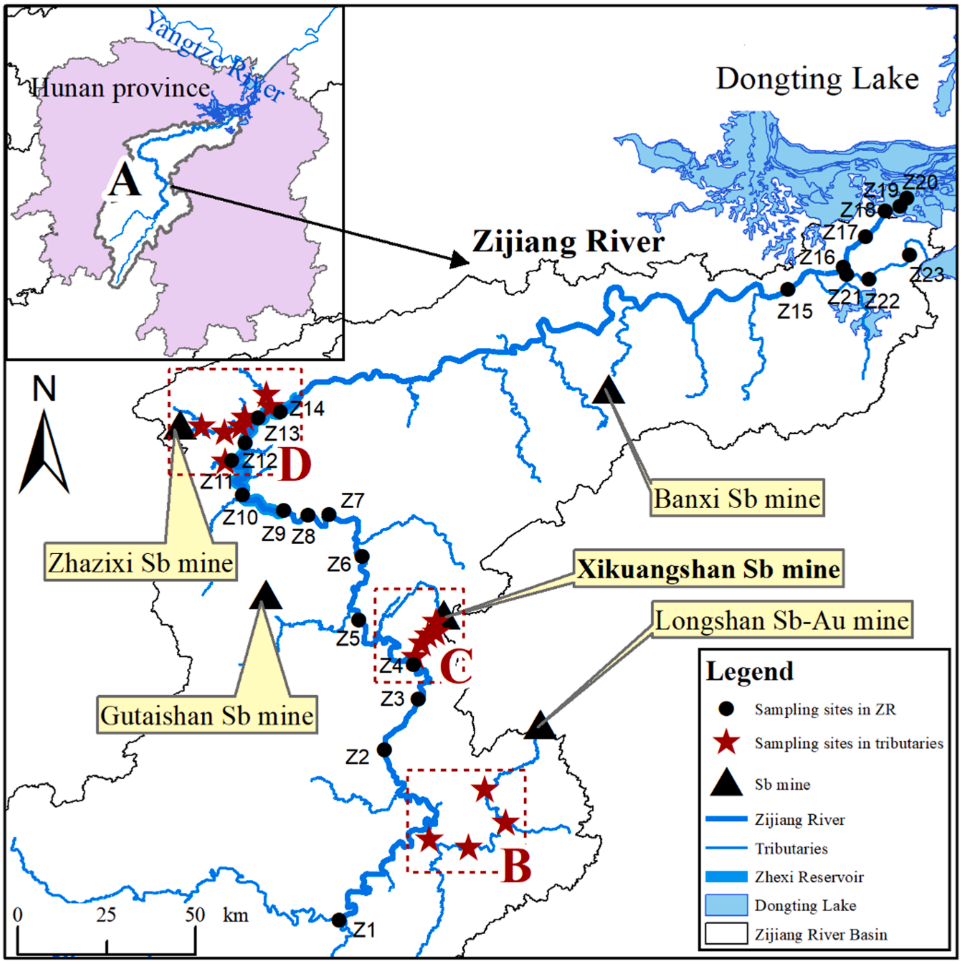

Fig. 1. Study area and sampling sites for sediments (A, the mainstream of the ZR; B, Longshan-Shaoshui River; C, Lianxi River; D, Creeks in the Zhexi Reservoir).

2. Materials and methods

2.1. Study area

The ZR is located in the transition zone between South China and the Yangtze River plate and has a total length of 653 km. The Nanshui River and Fuyi River flow into it at Shuangjiangkou in Shaoyang County, and it passes through Shaoyang, Lengshuijiang, Xinhua, Anhua, Taojiang, Yiyang, and finally into Dongting Lake. Typical large Sb deposits along the river in the ZR Basin include the Longshan (Sb-Au), Xikuangshan, Gutaishan, Zhazixi and Banxi mines (Fig. 1), and the reserves and genetic types of the Sb deposits are shown in Table S1. The mineral composition is simple, with stibnite being the main ore mineral, which is associated with trace amounts of pyrite, arsenopyrite, pyrite, and sphalerite. These Sb mines are all located in mountainous regions from which the rivers belonging to the ZR system originate. More than one hundred years of mining activities have been carried out in the basin, which has resulted in the production of large amounts of solid waste, such as waste rocks and residues from mining and smelting, and these flow into the ZR through tributaries (Liu et al., 2023).

2.2. Sample collection and analysis

2.2.1. Sample collection

In April 2021, in the mainstream of the ZR (area A) and in tributaries near Sb mines included the Longshan-Shaoshui River (area B), Lianxi River (area C) and Creeks in the Zhexi Reservoir (area D), 23, 4, 5 and 7 sediment samples were separately collected using grab buckets, stored in polyethylene ziplock bags and sealed in stainless steel lunch boxes. In the laboratory, the samples were freeze-dried, ground and sieved (< 200 mesh) and stored in polyethylene ziplock bags.

2.2.2. Analysis of total concentration of elements and chemical composition of Sb

According to the HJ 680−2013 standard method, 8 ml of digestion solution (6 ml HCl and 2 ml HNO_3) was placed in a digestion tank with ~0.2 g of sample for digestion by a microwave digestion instrument (Multiwave PRO, Anton Paar). The total Sb in the digestion solution was determined using a Hydride Deneration-Atomic Fluorescence Spectrometer (HG-AFS, AFS-9710, Beijing Haiguang Company), and the detection limit was 0.02 mg/kg. The concentrations of other elements in the HNO_3—$HClO_4$—HF mixed digest were analyzed by Inductively Coupled Plasma-Optical Emission Spectrometry (ICP-OES, ICAP-7400, Thermo Fisher, USA). More details on sample handling can be found in Liu et al. (2023).

According to the BCR procedure (Rauret et al., 1998), the different chemical forms of Sb in the sediments were extracted sequentially in four steps. Before sequentially adding the extractant, approximately 1 g of dry sample was weighed in a 50 ml centrifuge tube, and the extracted residue was washed three times with deionized water, freeze-dried, weighed, and digested using the same procedure used for the total concentration. The fractions obtained after BCR extraction were acid-soluble (F_1), reducible (F_2), oxidizable (F_3), and residual (F_4), where the value of $F_1 + F_2 + F_3$ represented the bioavailable concentration.

2.2.3. Purification and isotopic analysis of Sb

Antimony isotope sample digestion and analysis were completed at the State Key Laboratory of Environmental Geochemistry, Institute of Geochemistry, Chinese Academy of Sciences, using a two-step chromatographic purification process according to a method developed by Sun et al. (2021) (see Table S2 for details) to pretreat the digestion solution for Sb isotope analysis by MC-ICP-MS. An Sb-containing solution (NIST SRM 3102a) produced by the National Institute of Standards and Technology was selected as the reference standard for Sb isotopic analysis. The instrument error was controlled by the sample standard surround method and element doping (SSB-ED), with an accuracy of 0.4 ε (2SD).

2.3. The representation of Sb isotope

The antimony isotopic analysis results are reported in ε^{123}Sb notation, where ε^{123}Sb is defined as the deviation between the ^{123}Sb/^{121}Sb ratio in the sample and the mean value of the ^{123}Sb/^{121}Sb ratio in the standard, in units per ‱ (ε):

$$\varepsilon^{123}Sb = \left[\frac{\left(^{123}Sb/^{121}Sb\right)_{sample}}{\left(^{123}Sb/^{121}Sb\right)_{standard}} - 1 \right] \times 10000 \tag{1}$$

Although the absolute values of ε^{123}Sb for Sb obtained in different studies cannot be compared because the authors used different internal Sb isotopic standards, we can normalize the Sb isotopic composition data of environmental samples in the literature related to NIST SRM 3102a (Feng et al., 2019; Sun et al., 2021). Refer to Text S1 for the details of the normalization process.

2.4. Enrichment factor (EF) and estimation of Sb concentrations from different sources

The enrichment factor (EF) method is an important means to distinguish the anthropogenic and natural sources. In the EF calculation, the Sb concentration is normalized by the concentration of elements mainly derived from natural sources (such as Al and Ti), which provides Sb enrichment relative to the natural background. This normalization eliminates the dilution effect caused by the increase of natural components such as quartz, carbonates, and organics (Shotyk et al., 2003; Liu et al., 2022). In this study, the Sb enrichment factor (EF_{Sb}) was normalized by Al and Ti:

$$EF_{Sb} = \frac{\left[\frac{\left(\frac{Sb}{Al}\right)_{sample}}{\left(\frac{Sb}{Al}\right)_{bcakground}} + \frac{\left(\frac{Sb}{Ti}\right)_{sample}}{\left(\frac{Sb}{Ti}\right)_{background}} \right]}{2} \tag{2}$$

where "background" means the natural background. EF = 1 indicates that Sb concentration is similar to the natural background, while EF > 1 corresponds to Sb enrichment. Here, we chose the background values in the ZR sediments investigated by Li and Zheng (1989), in which Sb, Al and Ti are 3.11 mg/kg, 58.89 g/kg and 2.80 g/kg, respectively.

To investigate the response of sediments to the spatial differences in human activities in the ZR, the natural and anthropogenic concentrations of Sb were calculated by the following equation (Shotyk et al., 2003):

$$Sb_n = \frac{Sb_{sample}}{EF} \tag{3}$$

$$Sb_a = Sb_{sample} - \frac{Sb_{sample}}{EF} \tag{4}$$

where Sb_n and Sb_a are the natural and anthropogenic concentrations of Sb in the sample, respectively.

2.5. Quality assurance and quality control

For digestion, two standard materials (GBW-07,309 and GBW-07,311) were used to control the quality of sediment analysis, with two blank samples and no less than 10 % parallel samples per batch for quality assurance and quality control. The recovery rate of Sb for standard materials ranged from 95.06 % to 119.09 %, and the standard deviation of repeated samples was less than 10 %. The average recovery of other trace elements ranged from 83.29 % to 107.31 %. The long-term reproducibility of isotopic measurements was assessed by repeated measurements of Afla-IGCAS standard solutions (ε^{123}Sb =2.81±0.38). The overall ε^{123}Sb average and uncertainty of NIST 2711a (soil) and GSD-11 (sediment) were 1.63 ± 0.28 ε (2SD, $n = 5$) and 1.70 ± 0.36 ε (2SD, $n = 5$), respectively, which agreed well with the previous study (Sun et al., 2021).

3. Results

3.1. *Physicochemical properties of surface sediments*

The physiochemical parameters of the sediments are listed in Table 1. The results showed that the pH value was 6.31–7.43, and the coefficient of variation was CV ≤ 4.85 %. The sediment organic matter (SOM) concentrations in the four areas were all low, with an average of 3.80–4.80 %, and the corresponding coefficient of variation was 23.27–54.33 %. The average concentrations of major elements in areas A, B and C were Al > Fe > Ca > Ti > Mn, and the average concentration of major elements in area D was Al > Fe > Ti > Ca > Mn. The concentration of amorphous alumina (Al_o) was lower than that of amorphous iron oxide (Fe_o), and the variation was largest in area C (Lianxi River), with coefficients of variation of 68.91 % and 106.75 %. The particle size composition of each area was dominated by clay and silt, of which clay (< 4 μm) accounted for 7.84 %–83.41 %, silt (4–63 μm) accounted for 10.60 %–76.51 %, and sand (≥ 63 μm) accounted for 0 %–60.55 %, among which the sand content had a large degree of variation, and the variation coefficients of the four areas were all ≥ 133.93 %. The single-factor variance results showed that in different areas, the mean Ca concentration in area C was significantly greater than the mean Ca concentration in other areas ($p \leq 0.05$), while the mean values of other physical and chemical properties did not show statistical differences ($p > 0.05$).

3.2. *Geochemical characteristics of Sb*

3.2.1. *The tributaries near Sb mines*

The Sb isotopic compositions (ε^{123}Sb) of areas B, C, and D ranged from 2.31–3.99 ε, 3.12–5.63 ε, and 1.14–2.91 ε, respectively, corresponding to Sb concentrations of 4.47–62.04 mg/kg, 111.52–817.68 mg/kg and 7.07–66.06 mg/kg (Fig. 2a and Table 1). In a single tributary, the Sb isotopic composition changed little, while the Sb concentration changed greatly, with coefficients of variation of ⟨ 36.34 % and ⟩ 96.96 %, which indicates that there are differences in the geochemical behavior of Sb affected by mining activities in the ZR Basin, and that Sb isotopic variations are important in river systems. LX-3 and YTX-1 in areas C and D had the highest and lowest ε^{123}Sb values (5.63 ε and 1.14 ε) measured in this study, while YTX-1 was the sampling site with the highest Sb concentration in area D. It is worth noting that both areas B and D showed the opposite trend in Sb isotopic characteristics and Sb concentration changes, i.e., lower Sb concentrations corresponded to higher ε^{123}Sb values. However, the Sb concentration in area C was significantly different from that in areas B and D, and the isotopic composition of Sb in area C was significantly different from that in area D, which indicated that the isotopic signature of Sb changes during transfer from the original ore to the river.

Research showed that rivers affected by different types of mining areas and water samples from different aquifers exhibit various Sb isotopic characteristics (Resongles et al., 2015; Wen et al., 2023). Spatially, the ε^{123}Sb values of area B along the flow direction of the river showed that the ε^{123}Sb value increased from LS-1 to LS-3 and decreased at LS-4, which seemed to be affected by another tributary in this study (Fig. 3a). It is worth noting that LX3 in area C had the highest ε^{123}Sb, and the Sb concentration in the surface water of LX3 was very high, with an Sb concentration of 2373.38 μg/L, but the Sb concentration in the sediment was relatively low at 183.35 mg/kg. LX-3 is located downstream of the Sb smelter, mining plant and waste rock pile. After the Lianmeng Creek

Table 1
Basic physicochemical properties, concentrations of metals, and Sb isotopes in surface sediments.

Sb mine	River		pH	SOM %	Clay %	Silt %	Sand %	Al_o g/kg	Fe_o g/kg	Al g/kg	Fe g/kg	Mn g/kg	Ti g/kg	Ca g/kg	Sb mg/kg	As mg/kg	ε^{123}Sb ε
	Mainstream of the Zijiang River (ZR, A)	Min	6.31	1.40	7.84	10.60	0.00	0.43	1.48	16.30	13.27	0.28	3.19	2.09	3.86	11.42	0.50
	($n = 23$)	Max	7.43	8.89	83.41	76.51	60.55	5.64	25.72	134.56	59.17	2.89	5.36	16.81	133.63	74.53	3.13
		Mean	6.81	4.74	50.81	40.52	8.67	2.68	11.24	81.11	34.62	1.15	4.05	6.12	32.13	31.50	1.84
		CV (%)	4.85	39.90	36.02	37.63	151.32	51.32	46.72	33.41	23.76	42.90	14.87	65.68	100.16	48.35	36.14
Longshan Sb-Au mine	Longshan-Shaoshui River (B)	Min	6.81	2.95	21.83	35.34	0	0.72	1.48	50.96	28.85	0.59	4.21	1.42	4.47	19.96	2.31
	($n = 4$)	Max	7.14	8.67	64.66	56.46	21.71	2.54	13.54	121.44	40.93	5.08	5.45	41.85	62.04	36.87	3.99
		Mean	7.02	4.8	43.35	49.24	7.41	1.36	8.79	88.9	34.91	1.75	4.69	15.82	25.91	28.73	3.07
		CV (%)	2.07	54.33	40.46	19.53	138.13	60.68	60.34	35.43	16.78	127.05	12.61	117.76	96.63	26.84	24.93
Xikuangshan Sb mine	Lianxi River (C)	Min	6.95	3.25	16.05	36.30	0.00	0.57	1.54	46.29	24.37	0.45	3.05	4.97	111.52	33.99	2.12
	($n = 5$)	Max	7.15	7.23	63.70	69.10	27.59	2.87	31.89	134.69	48.20	1.06	6.05	100.42	817.68	189.78	5.63
		Mean	7.04	4.52	44.31	47.18	8.51	1.44	12.29	92.88	37.85	0.76	4.31	46.89	488.29	102.89	3.53
		CV (%)	1.36	35.34	52.22	28.47	146.24	68.91	106.75	36.44	26.16	36.83	29.27	91.10	67.65	60.56	36.33
Zhazixi Sb mine	Creeks in the Zhexi Reservoir (D)	Min	6.43	2.67	15.68	28.90	0.66	0.96	4.71	60.58	27.51	0.61	4.07	1.35	7.07	12.49	1.14
	($n = 7$)	Max	7.21	5.01	61.33	61.83	47.28	3.44	9.48	98.83	31.14	0.91	5.83	4.02	66.06	21.43	2.91
		Mean	6.72	3.80	43.93	43.39	12.68	2.08	6.92	73.02	29.16	0.73	4.69	2.72	28.17	15.74	2.03
		CV (%)	4.62	23.27	37.62	23.91	133.93	46.34	25.17	16.46	4.79	16.06	12.48	36.38	84.31	22.57	36.34

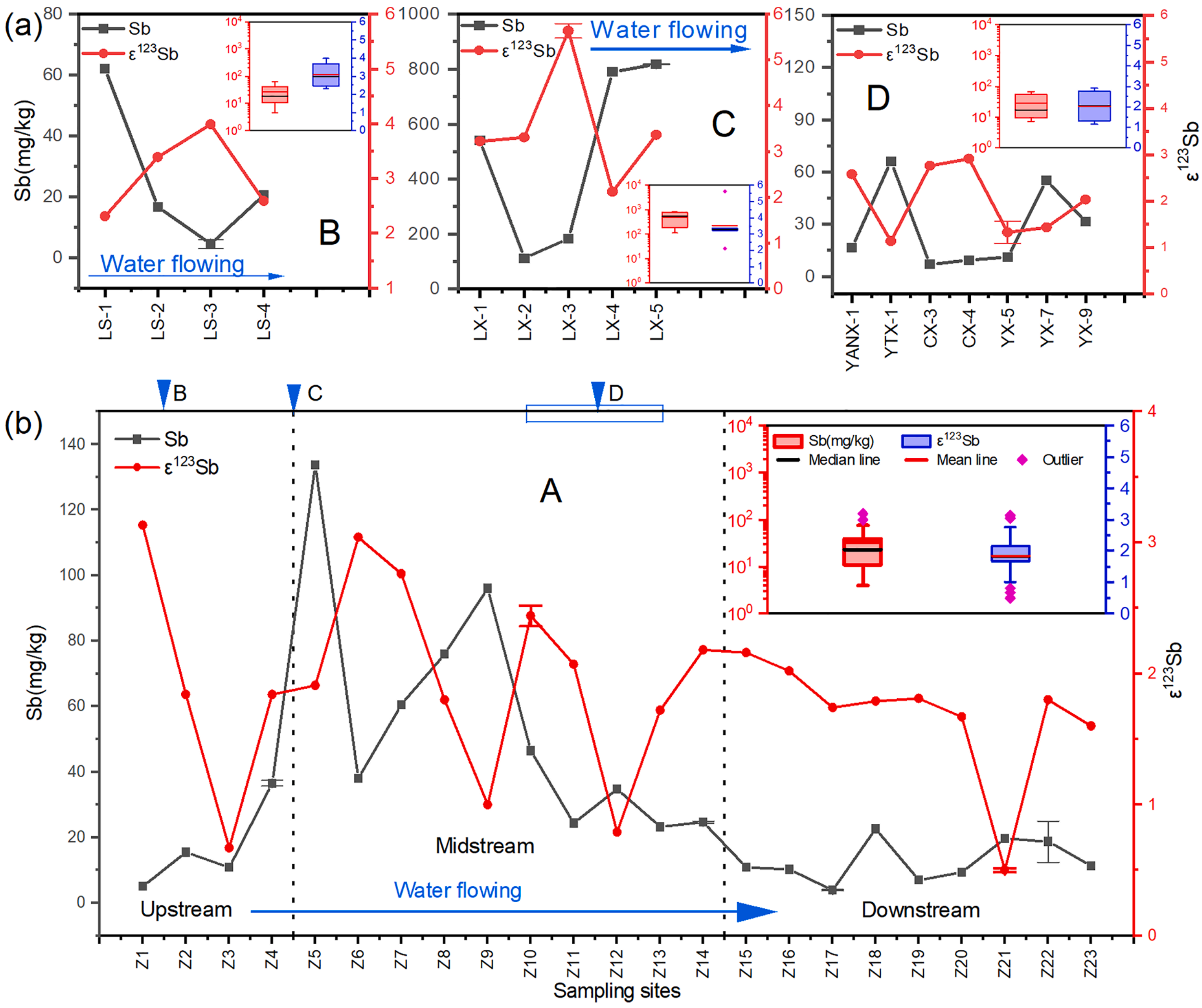

Fig. 2. Diagram of variations in Sb concentrations and ε^{123}Sb values in (a) tributaries near Sb mines (B, Longshan-Shaoshui River; C, Lianxi River; D, Creeks in the Zhexi Reservoir) and (b) the mainstream of the ZR (A). The boxplots show the statistical results of Sb and ε^{123}Sb respectively.

entered the Lianxi River, ε^{123}Sb at LX-2 slightly increased (Fig. 3b). In area D, the ε^{123}Sb values of Yangxi and Chanxi increased before they flowed into the ZR (Fig. 3c).

3.2.2. *The mainstream of the ZR*

In area A, the fluctuations in Sb concentration and isotopes were obvious upstream (Z1–Z4) and midstream (Z5–Z14), but the values were consistent downstream (Z15–Z23) (Fig. 2b). Although the one-way ANOVA results showed that the concentration of Sb in the sediments of the ZR was only significantly different from that of the Lianxi River ($p \leq 0.05$), the Sb isotopic composition in the ZR sediment was significantly different from that of the tributaries near Sb mines ($p \leq 0.05$), and its measured Sb isotopic composition (1.84 ± 0.66) was lower than the values obtained along the Longshan-Shaoshui River (3.07 ± 0.77) and the Lianxi River (3.53 ± 1.28). In similar regional studies, the downstream river waters did not show obvious fractionation relative to the mining river water (Resongles et al., 2015). In most of the sampling sites in the mainstream of the ZR, the trends in ε^{123}Sb and Sb concentrations were opposite to one another, but at sampling site Z5, which was affected by area C, this relationship was not obvious, indicating that mining input from Xikuangshan was the main source of Sb in the ZR, but Sb isotopic fractionation occurred in the river. For sampling sites affected by areas B and D, the changes in Sb concentration were not obvious, indicating that the diluting effect of the river can offset the impact of Sb input in these two areas, i.e., the Sb concentrations in sampling sites LS-4 and YX-9 were only 20.52 mg/kg and 31.55 mg/kg, respectively, while the Sb concentration in LX-5 in area C reached 817.68 mg/kg, which was 25 times the average Sb concentration in the ZR.

A summary of the Sb isotopic composition (ε^{123}Sb) reported in this study and those reported in other literature is shown in Fig. 4. The ε^{123}Sb value in environmental samples such as the river water in a study by Rouxel et al. (2003) and the seawater in a study by Resongles et al. (2015) after normalization by Eq. S1-S5 (Text S1) (Fig. 4b) was not significantly different from that in the original data (Fig. 4a), which showed that the original Sb isotopic fingerprint data could provide indirect information.

3.3. *The enrichment of Sb in surface sediments*

3.3.1. *Evidence for anthropogenic Sb import*

The results showed that the EF_{Sb} in the sediments from area A were 0.98–25.90, with an average value of 7.78 ± 7.34. Except for the EF_{Sb} of Z1 and Z17, which were ≈1, the EF_{Sb} at the sites were all > 1 (Fig. 5a), indicating that relative to the natural background, anthropogenic Sb was enriched in sediments. Spatially, the EF_{Sb} values were < 7.25 in the upstream region, followed by a large range of variation in the midstream (5.51–25.90), and finally small variation was observed in the

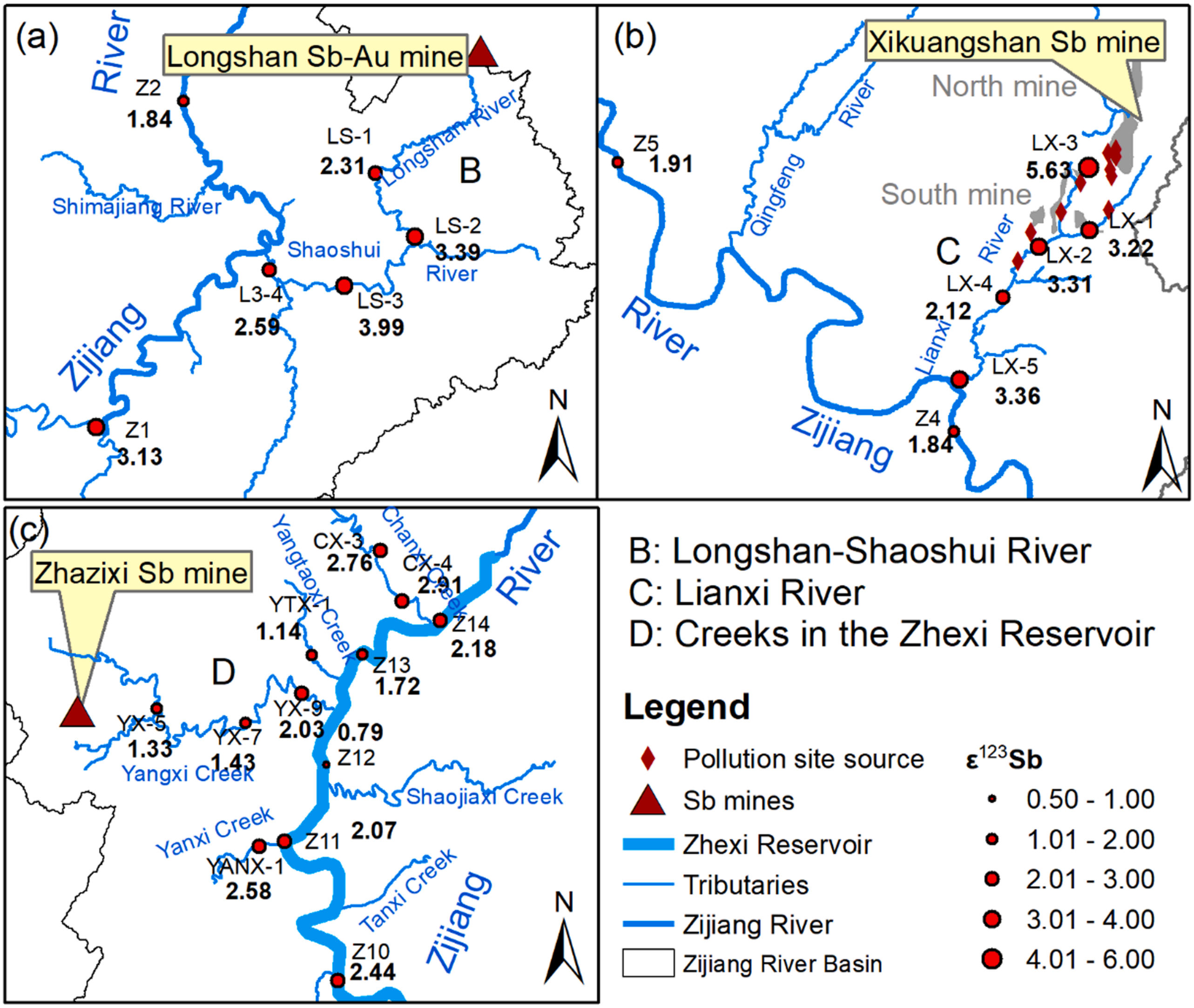

Fig. 3. The spatial distributions of the ε^{123}Sb value in sediments from the tributaries near Sb mines. (a) B, Longshan-Shaoshui River; (b) C, Lianxi River; and (c) Creeks in the Zhexi Reservoir.

downstream region (1.10–5.59). This was due to the high intensity of Sb mining and smelting activities in the upstream and midstream, as well as the sediment interception by Zhexi Dam (located at the junction of the midstream and downstream), resulting in significantly higher Sb pollution in the upstream and midstream than that in the downstream (Liu et al., 2023). Similarly, in tributaries near Sb mines, except for LS-3, the EF_{Sb} values of the sampling sites are all > 1 (Table S3), indicating that there was significant anthropogenic enrichment of Sb. Among them, EF_{Sb} of sediments in Lianxi River (area C) located in Xikuangshan Sb mine was the highest, ranging from 18.76 to 211.61.

3.3.2. The contribution of natural and anthropogenic sources of Sb

In general, the Sb in the tributaries near Sb mines and the mainstream of the ZR was mainly anthropogenic in origin (Table S3 and Fig. 5b). Fig. 5a showed that surface sediments with a high concentration of Sb_a were mainly distributed in the ZR, which was consistent with the distribution of EF. In the midstream of ZR, the highest concentration of Sb_a did not correspond to the highest EF value at Z9 but appeared at the second highest EF value at Z5 (Fig. 5b), which was strongly affected by high-concentration Sb input from Xikuangshan. Although the contributions of Sb_n and Sb_a in the ZR were 3.86 %–100 % and 0 %–96.14 %, respectively, in most of the samples, the contribution of anthropogenic sources (> 50 %) was greater than that of natural sources, especially in the midstream. As a metalloid that can be transported over long distances (Zhang et al., 2022), Sb is affected not only by large-scale Sb mining in this area but also by anthropogenic air emissions from the many Sb smelters present along the riverbank (Zhang et al., 2018). The light isotope (^{121}Sb) is enriched in the waste gas emitted by smelters, which shows that the fractionation of Sb in the ZR may also be affected by atmospheric anthropogenic sources. In this study, there was a significant correlation between Sb and Hg ($r = 0.73$, $p < 0.01$), indicating that the sources of both were largely the same, and according to the results of Hg isotope source analysis, the source of Hg in the ZR was mainly industrial anthropogenic sources, and atmospheric sources also had a small contribution (Mao et al., 2023).

3.4. Chemical composition of Sb

The BCR extraction results (Fig. 5c and Table S4) showed that in all surface sediments of the ZR, the fractions showed the trend $F_4 > F_2 > F_1 > F_3$. The Sb mainly existed in the residual fraction ($F_4 > 94.02$ %), and in the four regions, the average ratio of Sb in F_4 was 98.21 % (A), 95.85 % (B), 96.78 % (C) and 96.79 % (D), respectively, and the corresponding average concentration was 31.55 mg/kg (A), 24.56 mg/kg (B), 468.23 mg/kg (C) and 27.19 mg/kg (D), respectively. The percentage of bioavailable Sb in the surface sediments of the ZR was 0.89 %–3.08 %,

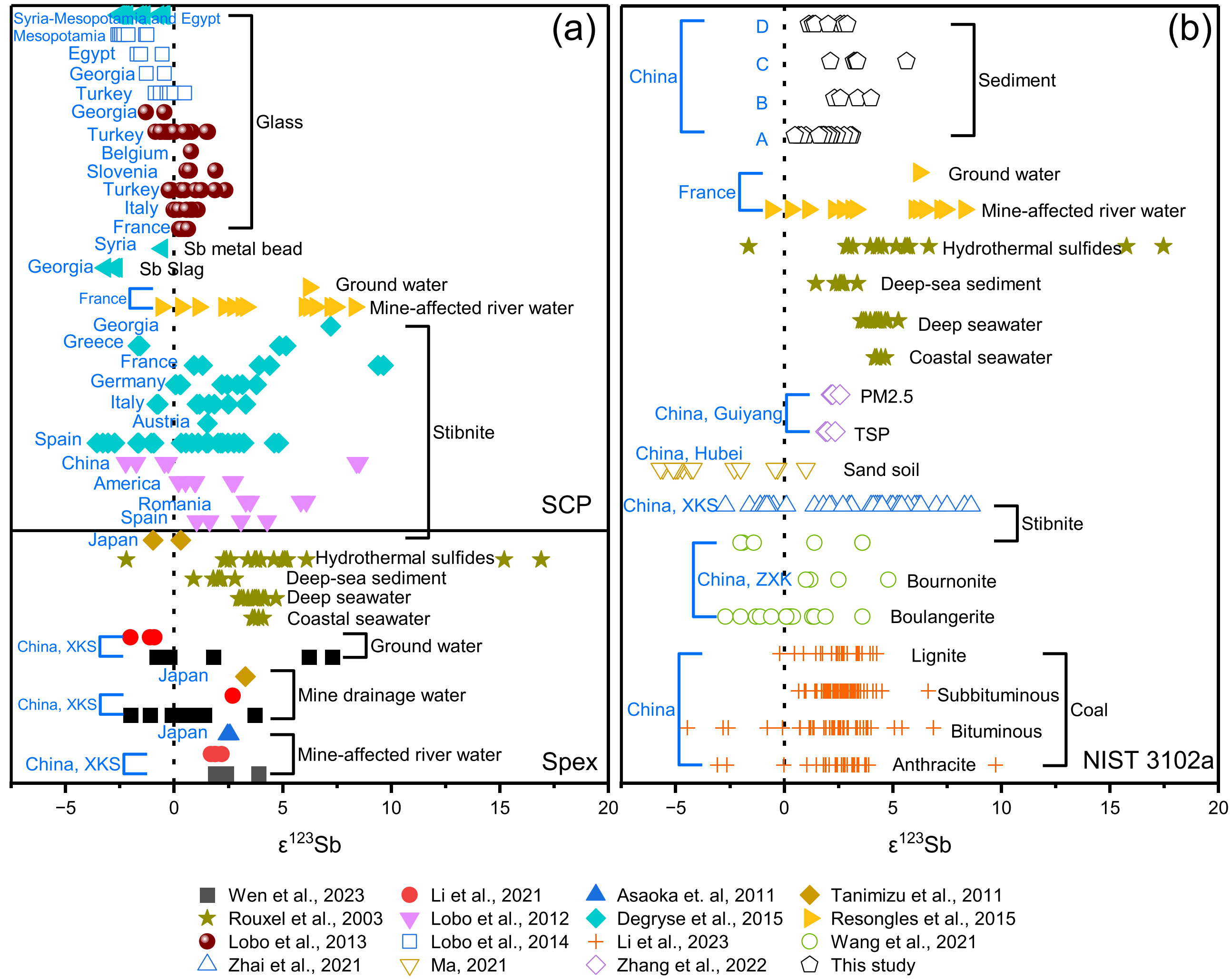

Fig. 4. Summary of ε^{123}Sb values in environmental samples reported in various studies (a) the Sb isotopic standards are SCP and Spex, and (b) the Sb isotopic standards are NIST 3102a (Rouxel et al., 2003; Asaoka et al., 2011; Tanimizu et al., 2011; Lobo et al., 2012, 2013, 2014; Degryse et al., 2015; Resongles et al., 2015; Li et al., 2021; Ma, 2021; Wang et al., 2021; Zhai et al., 2021; Zhang et al., 2022; Li et al., 2023; Wen et al., 2023).

corresponding to a concentration of 0.04−2.14 mg/kg. Under the control of total concentration (Liu et al., 2024), the concentrations of various fractions of Sb in sediments of Lianxi River were higher than those in other regions ($p < 0.05$). Overall, the proportion of effective state in sediments of tributaries in mining areas was higher than that in mainstream of ZR ($p < 0.05$). The low chemical mobility and bioavailability of Sb may be related to the fact that Sb easily combines with solid phases and has high stability (Johnston et al., 2020). In addition, studies have shown that under sulfidation and reduction conditions, Sb can be effectively isolated (Besold et al., 2019).

3.5. Correlations between Sb isotopes and other elements in sediments

This study conducted Spearman's correlation analysis on sediments of the mainstream and all sediments of ZR respectively, as shown in Table S5 and S6, and the results were basically consistent. There was no significant correlation between ε^{123}Sb in sediments and the concentrations of Sb and As ($p > 0.05$), and no other elements and physical and chemical properties were found to be correlated with ε^{123}Sb ($p > 0.05$). Although the four fractions of Sb were significantly positively correlated with total Sb concentration ($p \leq 0.01$), only the oxidizable fraction (F_3: mainly the part bound by organic matter) was found to be correlated with ε^{123}Sb ($r = 0.36$, $p \leq 0.05$). In addition, there was no significant correlation between biologically available Sb and ε^{123}Sb ($p > 0.05$).

4. Discussion

4.1. Comparison of Sb isotopic composition in different environmental media

This study is the first to report ε^{123}Sb in river sediments, and the observed ε^{123}Sb value was in the mid-range of all reported ε^{123}Sb values (Fig. 4), with extreme ε^{123}Sb values (0.50 and 5.63) recorded at the mouth of the ZR (Z21) and at the Lianxi River (LX-3) in Xikuangshan, where the main Sb ore mined is stibnite (Sb_2S_3). The range of Sb isotopic composition in this study was comparable to that of river surface water (Wen et al., 2023) affected by the Xikuangshan mine, but it was greater than that reported for Sb from the same site in the Xikuangshan mine (Zhai et al., 2021) and Zhaxikang mine in China (Wang et al., 2021) and other sites in other countries (Tanimizu et al., 2011; Lobo et al., 2012; Degryse et al., 2015). The stibnite samples have a narrower range than the ε^{123}Sb range reported for river water by Resongles et al. (2015). The contrasting features of these Sb-influenced streams may reflect local differences in the isotopic composition of stibnite, as other Sb-bearing minerals in the ore may also have contributed to the Sb isotopic signature in these streams (Resongles et al., 2015). Antimony ore smelting may also have produced residual slag with heavier Sb isotopic signatures, as seen for Hg (Yin et al., 2013) and Zn isotopes (Sivry et al., 2008). These slags may also have resulted in heavier Sb isotopes in the

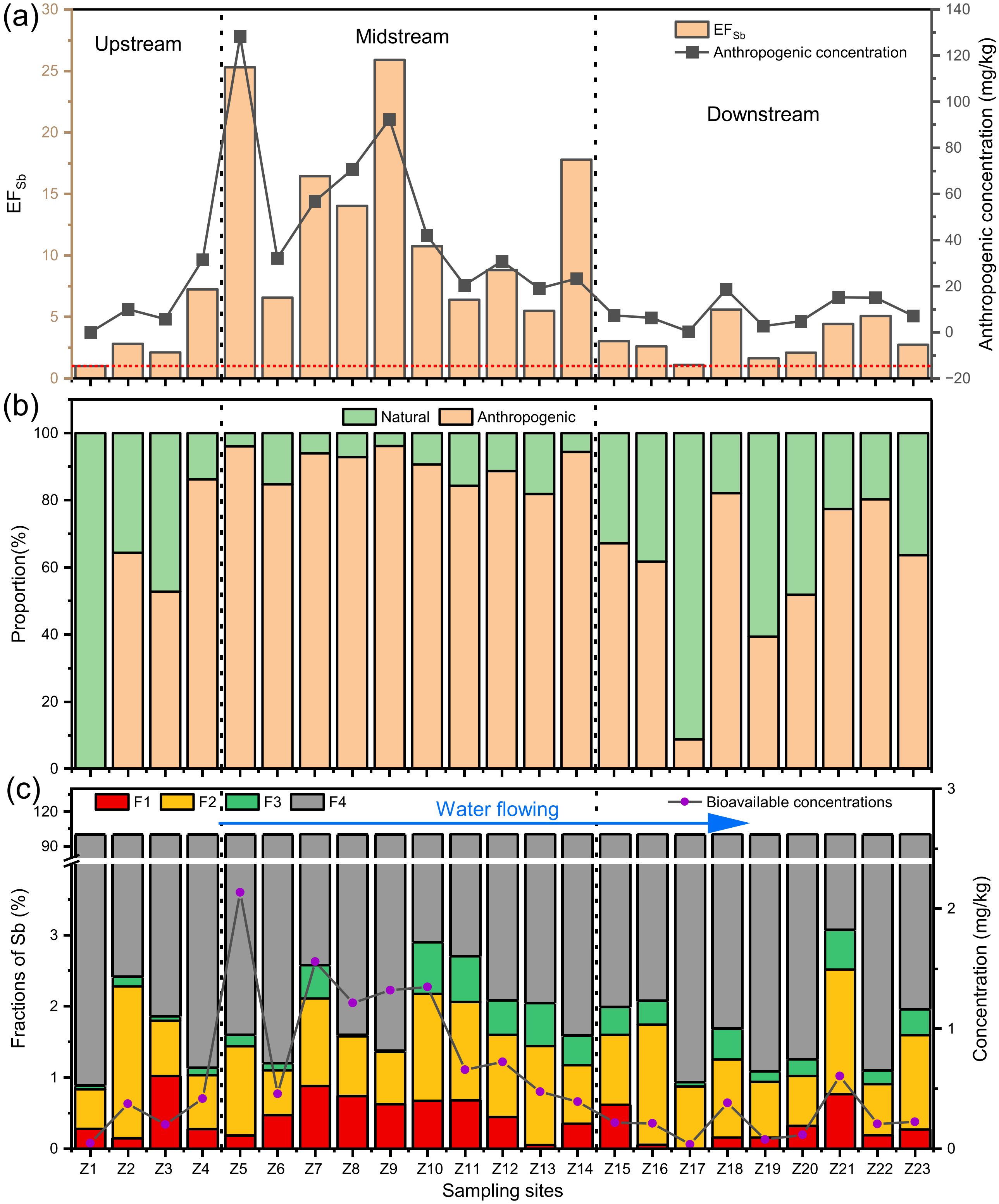

Fig. 5. (a) The enrichment factor (EF) and anthropogenic concentration of Sb, (b) the percentage of natural and anthropogenic sources of Sb, and (c) the percentages of chemical fractions and bioavailable concentrations of Sb based on BCR extractions in sediments from the mainstream of the ZR.

Sb-influenced rivers in areas B, C, and D. Alternatively, biogeochemical processes involved in the movement of Sb from the ore material to the water may have altered the initial Sb isotopic composition, and the presence of greater quantities of adsorbents (such as Fe-, Mn- and Al-(hyd)oxides and organic matter) in the sediments might have also had an effect. Therefore, Sb dynamics in sediments are more complex than those in surface water.

4.2. *The potential influencing factors of Sb isotopes*

The high Sb concentration and low ε^{123}Sb features in the surface sediments of the ZR suggested that Sb might be influenced by mining-derived deposition, as revealed by the high Zn concentration and low δ^{66}Zn studied in the karst regions of Southwest China (Xia et al., 2020). However, the behavior of Sb was also affected by environmental depositional conditions that affected its chemical distribution. It is not yet known whether chemical distribution affects the isotopic fractionation of Sb (Wen et al., 2018), but in this study, the correlation between the four fractions of Sb and ε^{123}Sb was not significant ($p > 0.05$) (Table S5), indicating that chemical distribution had little effect on Sb isotopic fractionation.

The biogeochemical process of Sb migration involves oxidation, dissolution, release, adsorption and the precipitation of stibnite (Sb_2S_3), which has a potential impact on the isotope composition and fractionation of antimony (Wang et al., 2021; Zhai et al., 2021). The fractionation of Sb isotopes during the dissolution of minerals such as stibnite has only been preliminarily studied (Ferrari et al., 2022). Most of the Sb in the ore was released during the washing process, so the Sb isotopic composition of the wastewater should be almost indistinguishable from that of the mineral, which may indirectly affect the river water affected by the pollution (Guo et al., 2014). In addition, Rouxel et al. (2003) emphasized that redox reactions can produce Sb isotopic fractionation. Laboratory adsorption studies of Sb(V) revealed that ferrihydrite preferentially adsorbed the ^{121}Sb isotope, thus slightly enriching the heavier isotope (^{123}Sb) in the aqueous phase (Araki et al., 2009). In a study with a geochemical background similar to the one in this study, Tanimizu et al. (2011) showed a 0.30 ‰ difference between stibnite in mine waste in Ichinokawa, Japan, and in the corresponding drainage, which was richer in the heavy ^{123}Sb isotope. This fractionation was related to the preferential adsorption of the ^{121}Sb isotope by ferric hydroxide. Therefore, the oxidation of Sb(III) and the adsorption or precipitation of Sb (III)/Sb(V) may contribute to Sb isotopic fractionation in the river in the mining area. This suggests that the various Sb isotopic compositions in tributaries near the Sb mines in this study (1.14–5.63 ε) may not be representative of the Sb signature in the original stibnite (−2.7–+8.6 ε) (Zhai et al., 2021) but instead arise from a combination of various geochemical processes that may occur at any stage of Sb transport from the mine to the river. According to the results of EF_{Sb} and of the bioavailability of Sb (Fig. 5a and 5c), the higher the concentration of the bioavailability, the higher the EF_{Sb}, indicating that the degree of human influence was also higher, and the ε^{123}Sb was also higher, although EF and Sb did not show a correlation overall ($p > 0.05$).

4.3. Sources and transport of Sb in sediments based on Sb isotopes

4.3.1. The tributaries near Sb mines

Although there is a lack of relevant studies on the characteristics of Sb isotopic fractionation in river sediments, studies on the characteristics of Sb isotopic fractionation and its migration in river water affected by mining are ongoing. Resongles et al. (2015) reported that the ε^{123}Sb of the Gardon River decreased slightly past its confluence with the Alès River, while the ε^{123}Sb of the Gardon of the Anduze River increased slightly past its confluence with the Amous River. It indicated that Sb fractionation was limited in the river during transport, which is related to the dominant Sb form of Sb(V) (Resongles et al., 2015). The latest results of Wen et al. (2023) on Sb isotopes in Xikuangshan showed that the dilution of Sb along the river in the Xikuangshan stream (Feishuiyan) and the weak adsorption of Sb by Fe-Mn suspended particles and sediments does not lead to apparent Sb isotopic fractionation in river water. The physicochemical conditions, the predominance of Sb(V), the stable Sb isotopic composition, and the high Sb concentration suggest that Sb is conserved during transport in the Feishuiyan stream. Therefore, based on the above analyses, the ε^{123}Sb value and Sb concentration fluctuations in the sediments along the tributary flow direction in the studied mining area indicated that dilution of Sb along the river and weak adsorption of Sb by sediments do not lead to significant sediment Sb isotopic fractionation. However, the isotopic fractionation of Sb in sediments may increase during migration from the pollution source along the river, and further research is needed on other possible sources of Sb and unknown geochemical background values. It should be noted that compared with the ε^{123}Sb of the Feishuiyan stream waters (1.9–3.9 ε) reported by Wen et al. (2023), the ε^{123}Sb of the Lianxi River sediments in this study is relatively higher, which may be related to regional background and differences in Sb isotope reference standards (Sun et al., 2021). In addition, the contrasting features of ε^{123}Sb in the sediments from the tributaries near Sb mines in this study may reflect the background value of the local isotopic composition, including differences in the composition of Sb ore, because the Sb ore present in auxiliary minerals may also contribute to the ε^{123}Sb signature of these tributaries (Resongles et al., 2015). Therefore, Sb isotopes help track the source of Sb pollution in river systems far from mining areas. In addition, Fig. 6a, 7b and 7c showed that the δ^{202}Hg in the sediment of the Lianxi River located in Xikuangshan was also significantly higher than that in the ZR, and Mao et al. (2023) successfully used Hg isotopes to analyze the source of Hg in the sediments of the Lianxi River, and nonferrous metal smelting was the main industrial contributor to the Lianxi River.

4.3.2. The mainstream of the ZR

The Sb concentration in surface waters from the ZR was much lower than that in surface waters of the tributaries near Sb mines, but this characteristic was not shown in sediments (Liu et al., 2023), which may be because the deposition conditions of ZR are better than those of tributaries near Sb mines, resulting in this difference (Feyte et al., 2010; Xi et al., 2013). The Sb isotopic signature of sediments is likely to be mainly controlled by the stock size and isotopic signature of potential sources. Furthermore, a prerequisite for using stable metal isotopes as metal source tracers in conservative systems is that mixing needs to be the result of changes in stable metal isotopes, with limited additional fractionation effects (adsorption, complexation, coprecipitation, etc.) (Zhong et al., 2021).

The Sb concentration in sediments from the ZR was positively correlated with the abundance of Fe_o and Al_o (Liu et al., 2023), and this strong influence of Fe and Al on Sb suggests that Sb is associated with Fe-Al oxides, which indicates the role of Fe-Al oxides on Sb migration. However, due to the significant influence of Sb mining, the migration of Sb in sediments from the tributaries near Sb mines is no longer mainly controlled by Fe-Al oxides but is related to the anthropogenic inputs caused by mining and smelting activities (Liu et al., 2023). Spatially, the concentration of Sb was basically consistent with the distribution of ε^{123}Sb in the midstream, while there is a large difference between the upstream and the downstream (Fig. S1). We also found that there is no significant correlation between the ε^{123}Sb value and other physiochemical factors (Table S5 and S6), and the Fe-Al oxides related to Sb have little effect on ε^{123}Sb, which indicates that adsorption has little influence on the metal isotopes present in natural environments. The contribution of fractionation is very small, which was also demonstrated by Zhou et al. (2022) in an experiment involving Sb adsorption to aluminum oxide.

In general, the ε^{123}Sb value in the sediments of the ZR is significantly smaller than the ε^{123}Sb value in the tributaries near Sb mines. Similarly, in a study by Wen et al. (2023), the ε^{123}Sb value of river surface water at a sampling site affected by slag-leaching water was significantly higher than that at other sampling sites. The values of ε^{123}Sb in the upstream, midstream and downstream regions of the ZR were 1.87 ε, 1.97 ε and 1.68 ε, respectively, and the highest ε^{123}Sb value appeared in midstream, which showed that the Sb isotopic fractionation in the midstream region was affected by the high ε^{123}Sb value from the mining area. Fig. 6d showed that after the Lianxi River and Qingfeng River flowed into the ZR, the ε^{123}Sb values from Z4 (1.84 ε) to Z5 (1.91 ε) increased slightly. According to the overall trends in ε^{123}Sb in the ZR, Sb was conserved during transport in the river. At the same time, according to the Sb isotope discriminant analysis results (Fig. 6d), the Sb isotopic signature at most of the sampling sites matches that of the original area, which further confirms that Sb isotopes in the ZR undergo limited

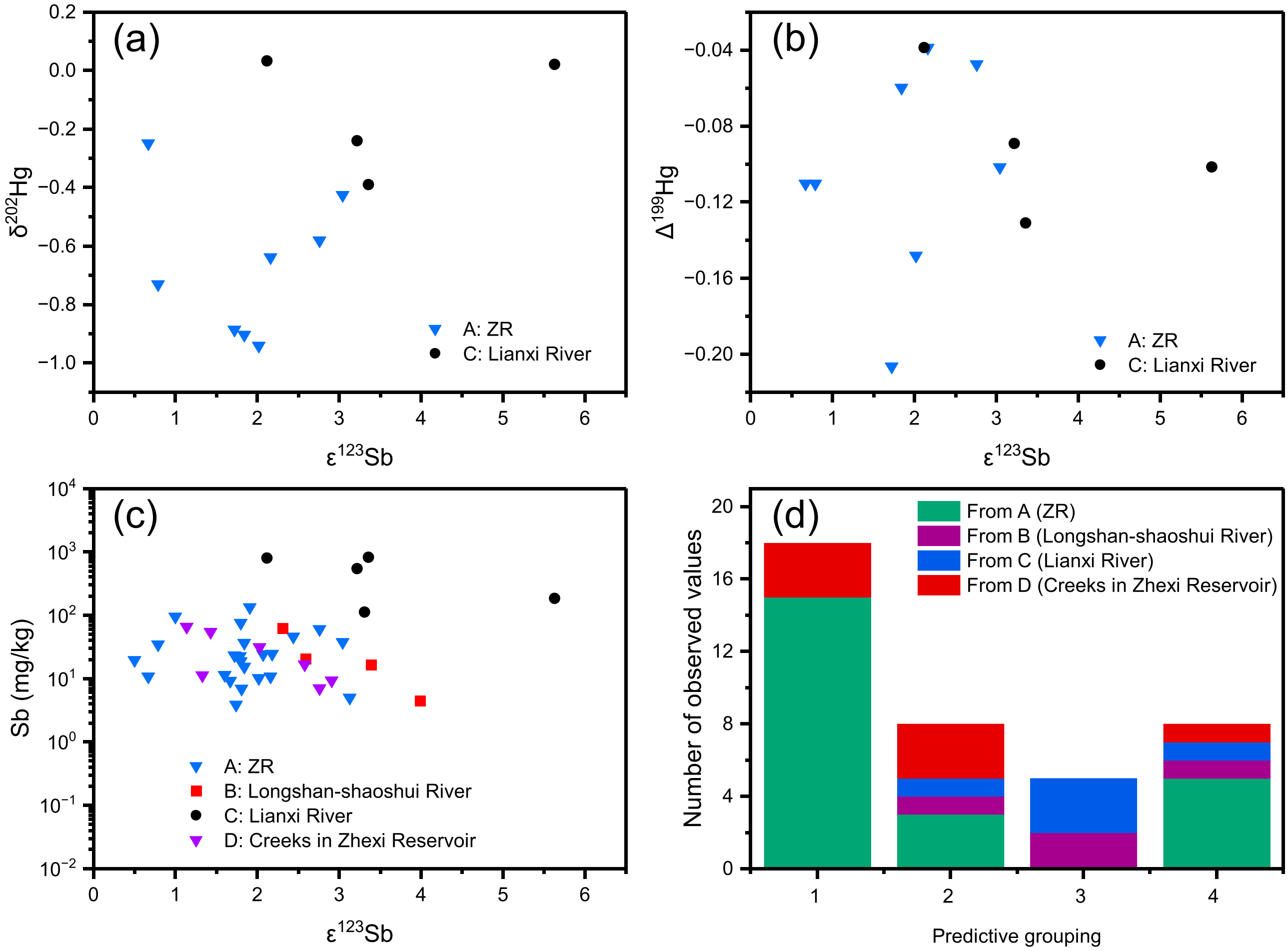

Fig. 6. Scatter plots of (a) ε^{123}Sb vs. δ^{202}Hg, (b) ε^{123}Sb vs. Δ^{199}Hg and (c) ε^{123}Sb vs. Sb concentrations; (d) the results of ε^{123}Sb discriminant analysis.

fractionation during migration in the sediment, so the Sb isotopic signature can be used for surface sediment tracing to find the source of Sb.

Overall, we conclude that the closer a site is to the mining area, the more active the Sb migration, and mining activities bring subsurface heavy metals to the surface, thereby enhancing their activity under unique hydrogeological conditions. The absolute concentration of Sb during mining is higher, and the amount of leached Sb increases correspondingly, which is associated with leaching-related release. Fe-Al oxides can affect the migration of Sb in the ZR, but they do not have a significant impact on Sb isotopic fractionation.

5. Conclusion

In this study, the Sb isotopic composition in hydrologic sediments affected by different mining areas was determined for the first time through the analysis of ε^{123}Sb values. The results showed that there were obvious changes in the Sb isotopic composition in the sediments of different areas in the ZR Basin, and the value of ε^{123}Sb in the sediments of the ZR was significantly smaller than the value of ε^{123}Sb in the tributaries near Sb mines. Dilution of Sb along rivers did not lead to significant Sb isotopic fractionation in sediments, and Sb was conserved during transport along rivers. The ZR Basin was strongly affected by human activities, and there was obvious anthropogenic Sb enrichment. Although mining activities (especially in the midstream) could increase Sb migration in the sediments from the ZR under special hydrogeological conditions where mine tributaries enter the mainstream, they had little effect on Sb isotope fractionation. Differences in the Sb isotopic composition in sediments indicated that it is a potentially useful tool for studying Sb sources and biogeochemical processes in hydrological systems. However, further studies on other possible sources of Sb isotopes and unknown geochemical background values are needed to better identify and characterize Sb isotopic fractionation resulting from different biogeochemical processes occurring during Sb release and transport in rivers.

CRediT authorship contribution statement

Huiji Liu: Writing – original draft, Validation, Software, Methodology, Investigation, Formal analysis, Data curation. **Guangyi Sun:** Validation, Formal analysis, Data curation. **Mengchang He:** Writing – review & editing, Supervision, Project administration, Investigation, Funding acquisition, Conceptualization. **Xinbin Feng:** Writing – review & editing, Methodology. **Chunye Lin:** Writing – review & editing, Investigation. **Wei Ouyang:** Writing – review & editing, Investigation. **Xitao Liu:** Writing – review & editing, Investigation.

Declaration of competing interest

The authors declare that they have no known competing financial interests or personal relationships that could have appeared to influence the work reported in this paper.

Data availability

Data will be made available on request.

Acknowledgments

This work was financially supported by the National Natural Science Foundation of China (No. 42030706).

Supplementary materials

Supplementary material associated with this article can be found, in the online version, at doi:10.1016/j.watres.2024.121427.

References

Araki, Y., Tanimizu, M., Takahashi, Y., 2009. Antimony isotopic fractionation during adsorption on ferrihydrite. Geochim. Cosmochim. Acta 73. A49-A49.

Asaoka, S., Takahashi, Y., Araki, Y., Tanimizu, M., 2011. Preconcentration method of antimony using modified thiol cotton fiber for isotopic analyses of antimony in natural samples. Anal. Sci. Int. J. Jpn. Soc. Anal. Chem. 27, 25–28. https://doi.org/10.2116/analsci.27.25.

Besold, J., Eberle, A., Noel, V., Kujala, K., Kumar, N., Scheinost, A.C., Pacheco, J.L., Fendorf, S., Planer-Friedrich, B., 2019. Antimonite binding to natural organic matter: spectroscopic evidence from a mine water impacted peatland. Environ. Sci. Technol. 53, 10792–10802. https://doi.org/10.1021/acs.est.9b03924.

Degryse, P., Lobo, L., Shortland, A., Vanhaecke, F., Blomme, A., Painter, J., Gimeno, D., Eremin, K., Greene, J., Kirk, S., Walton, M., 2015. Isotopic investigation into the raw materials of Late Bronze Age glass making. J. Archaeol. Sci. 62, 153–160. https://doi.org/10.1016/j.jas.2015.08.004.

Dillis, S., Van Ham-Meert, A., Leeming, P., Shortland, A., Gobejishvili, G., Abramishvili, M., Degryse, P., 2019. Antimony as a raw material in ancient metal and glass making: provenancing Georgian LBA metallic Sb by isotope analysis. STAR: Science & Technology of Archaeological Research 5, 98–112. https://doi.org/10.1080/20548923.2019.1681138.

Feng, L.P., Zhou, L., Liu, J.H., Hu, Z.C., Liu, Y.S., 2019. Determination of gallium isotopic compositions in reference materials. Geostand. Geoanal. Res. 43, 701–714. https://doi.org/10.1111/ggr.12294.

Ferrari, C., Meheut, M., Resongles, E., Freydier, R., Casiot, C., 2022. Equilibrium mass-dependent isotope fractionation of antimony between stibnite and Sb secondary minerals: A first-principles study. Chemical Geology 611. https://doi.org/10.1016/j.chemgeo.2022.121115.

Feyte, S., Tessier, A., Gobeil, C., Cossa, D., 2010. In situ adsorption of mercury, methylmercury and other elements by iron oxyhydroxides and organic matter in lake sediments. Applied Geochemistry 25, 984–995. https://doi.org/10.1016/j.apgeochem.2010.04.005.

Guo, X.J., Wang, K.P., He, M.C., Liu, Z.W., Yang, H.L., Li, S.S., 2014. Antimony smelting process generating solid wastes and dust: characterization and leaching behaviors. J. Environ. Sci. 26, 1549–1556. https://doi.org/10.1016/j.jes.2014.05.022.

He, M.C., Wang, N.N., Long, X.J., Zhang, C.J., Ma, C.L., Zhong, Q., Wang, A., Wang, Y., Pervaiz, A., Shan, J., 2019. Antimony speciation in the environment: Recent advances in understanding the biogeochemical processes and ecological effects. J. Environ. Sci. 75, 14–39. https://doi.org/10.1016/j.jes.2018.05.023.

He, M.C., Wang, X.Q., Wu, F.C., Fu, Z.Y., 2012. Antimony pollution in China. Science of the Total Environment 421-422, 41–50. https://doi.org/10.1016/j.scitotenv.2011.06.009.

Herath, I., Vithanage, M., Bundschuh, J., 2017. Antimony as a global dilemma: Geochemistry, mobility, fate and transport. Environmental Pollution 223, 545–559. https://doi.org/10.1016/j.envpol.2017.01.057.

Hoefs, J., 2018. Stable Isotope Geochemistry, Eighth Edition. Springer International Publishing, Switzerland.

Johnston, S.G., Bennett, W.W., Doriean, N., Hockmann, K., Karimian, N., Burton, E.D., 2020. Antimony and arsenic speciation, redox-cycling and contrasting mobility in a mining-impacted river system. Science of the Total Environment 710, 136354. https://doi.org/10.1016/j.scitotenv.2019.136354.

Krachler, M., Zheng, J., Koerner, R., Zdanowicz, C., Fisher, D., Shotyk, W., 2005. Increasing atmospheric antimony contamination in the northern hemisphere: snow and ice evidence from Devon Island, Arctic Canada. J. Environ. Monit. 7, 1169–1176. https://doi.org/10.1039/b509373b.

Li, J., Zheng, C.J., 1989. The Handbook of Environmental Background Values in China. Environmental Science Press of China, Beijing, pp. 379–387 in Chinese.

Li, S., Deng, Y., Zheng, H., Liu, X., Tang, P., Zhou, J., Zhu, Z., 2021. A new purification method based on a thiol silica column for high precision antimony isotope measurements. J. Anal. Atom. Spectrom. 36, 157–164. https://doi.org/10.1039/d0ja00367k.

Li, X., Sun, G., Wu, Y., Zhou, M., Li, Z., Bi, X., Huang, J.H., Feng, X., 2023. Origin and geochemical significance of antimony in Chinese coal. Int. J. Coal. Geol. 265, 104165 https://doi.org/10.1016/j.coal.2022.104165.

Liu, H.J., Liu, E.F., Yu, Z.Z., Lin, Q., Zhang, E.L., Shen, J., 2022. Spatio-temporal accumulation patterns of trace metals in sediments of a large plateau lake (Erhai) in Southwest China and their relationship with human activities over the past century. J. Geochem. Explor. 234, 106943 https://doi.org/10.1016/j.gexplo.2022.106943.

Liu, H.J., Zeng, W., He, M.C., Lin, C.Y., Ouyang, W., Liu, X.T., 2023. Occurrence, distribution, and migration of antimony in the Zijiang River around a superlarge antimony deposit zone. Environmental Pollution 316, 120520. https://doi.org/10.1016/j.envpol.2022.120520.

Liu, H.J., Zeng, W., Lai, Z.Y., He, M.C., Lin, C.Y., Ouyang, W., Liu, X.T., 2024. Comparison of antimony and arsenic behaviour at the river-lake junction in the middle of the Yangtze River Basin. J. Environ. Sci. 136, 189–200. https://doi.org/10.1016/j.jes.2023.02.028.

Liu, J.F., Chen, J.B., Zhang, T., Wang, Y.N., Yuan, W., Lang, Y.C., Tu, C.L., Liu, L.Z., Birck, J.L., 2020. Chromatographic purification of antimony for accurate isotope analysis by MC-ICP-MS. J. Anal. Atom. Spectrom. 35, 1360–1367. https://doi.org/10.1039/D0JA00136H.

Lobo, L., Degryse, P., Shortland, A., Eremind, K., Vanhaeckea, F., 2014. Copper and antimony isotopic analysis via multicollector ICP-mass spectrometry for provenancing ancient glass. J. Anal. Atom. Spectrom. 29, 58–64. https://doi.org/10.1039/c3ja50303h.

Lobo, L., Degryse, P., Shortland, A., Vanhaecke, F., 2013. Isotopic analysis of antimony using multi-collector ICP-mass spectrometry for provenance determination of Roman glass. J. Anal. Atom. Spectrom. 28, 1213–1219. https://doi.org/10.1039/c3ja50018g.

Lobo, L., Devulder, V., Degryse, P., Vanhaecke, F., 2012. Investigation of natural isotopic variation of Sb in stibnite ores via multi-collector ICP-mass spectrometry – perspectives for Sb isotopic analysis of Roman glass. J. Anal. Atom. Spectrom. 27 https://doi.org/10.1039/c2ja30062a.

Ma, Y.W., 2021. Optimization of Method For Determining Antimony Stable Isotopes and Its Preliminary Application. China University of Geosciences (Beijing), Beijing in Chinese.

Mao, L., Ren, W., Liu, X., He, M., Lin, C., Zhong, Y., Tang, Y., Ouyang, W., 2023a. Tracking the multiple Hg sources in sediments in a typical river-lake basin by isotope compositions and mixing models. J. Hazard. Mater. 459 https://doi.org/10.1016/j.jhazmat.2023.132166.

Rauret, G., López-Sánchez, J.F., Sahuquillo, A., Rubio, R., Davidson, C., Ureb, A., Quevauviller, P., 1998. Improvement of the BCR three step sequential extraction procedure prior to the certification of new sediment and soil reference materials. J. Environ. Monit. 1, 57–61. https://doi.org/10.1039/A807854H.

Resongles, E., Freydier, R., Casiot, C., Viers, J., Chmeleff, J., Elbaz-Poulichet, F., 2015. Antimony isotopic composition in river waters affected by ancient mining activity. Talanta 144, 851–861. https://doi.org/10.1016/j.talanta.2015.07.013.

Rouxel, O., Ludden, J., Fouquet, Y., 2003. Antimony isotope variations in natural systems and implications for their use as geochemical tracers. Chemical Geology 200, 25–40. https://doi.org/10.1016/s0009-2541(03)00121-9.

Sen, I.S., Peucker-Ehrenbrink, B., 2012. Anthropogenic Disturbance of Element Cycles at the Earth's Surface. Environ. Sci. Technol. 46, 8601–8609. https://doi.org/10.1021/es301261x.

Shotyk, W., Goodsite, M.E., Roos-Barraclough, F., Frei, R., Heinemeier, J., Asmund, G., Lohse, C., Hansen, T.S., 2003. Anthropogenic contributions to atmospheric Hg, Pb and As accumulation recorded by peat cores from southern Greenland and Denmark dated using the ^{14}C "bomb pulse curve". Geochim. Cosmochim. Acta 67, 3991–4011. https://doi.org/10.1016/S0016-7037(03)00409-5.

Sivry, Y., Riotte, J., Sonke, J.E., Audry, S., Schäfer, J., Viers, J., Blanc, G., Freydier, R., Dupré, B., 2008. Zn isotopes as tracers of anthropogenic pollution from Zn-ore smelters The Riou Mort–Lot River system. Chemical Geology 255, 295–304. https://doi.org/10.1016/j.chemgeo.2008.06.038.

Sun, G., Wu, Y., Feng, X., Wu, X., Li, X., Deng, Q., Wang, F., Fu, X., 2021. Precise analysis of antimony isotopic composition in geochemical materials by MC-ICP-MS. Chemical Geology 582, 120459. https://doi.org/10.1016/j.chemgeo.2021.120459.

Tanimizu, M., Araki, Y., Asaoka, S., Takahashi, Y., 2011. Determination of natural isotopic variation in antimony using inductively coupled plasma mass spectrometry for an uncertainty estimation of the standard atomic weight of antimony. Geochem. J. 45, 27–32. https://doi.org/10.2343/geochemj.1.0088.

Wang, D., Mathur, R., Zheng, Y., Qiu, K., Wu, H., 2021. Redox-controlled antimony isotope fractionation in the epithermal system: New insights from a multiple metal stable isotopic combination study of the Zhaxikang Sb-Pb-Zn-Ag deposit in Southern Tibet. Chemical Geology 584, 120541. https://doi.org/10.1016/j.chemgeo.2021.120541.

Wang, X.Q., He, M.C., Xi, J.H., Lu, X.F., 2011. Antimony distribution and mobility in rivers around the world's largest antimony mine of Xikuangshan, Hunan Province, China. Microchem. J. 97, 4–11. https://doi.org/10.1016/j.microc.2010.05.011.

Wehmeier, S., Ellam, R., Feldmann, J., 2003. Isotope ratio determination of antimony from the transient signal of trimethylstibine by GC-MC-ICP-MS and GC-ICP-TOF-MS. J. Anal. Atom. Spectrom. 18 https://doi.org/10.1039/b302242k.

Wen, B., Zhou, J., Jia, X., Zhou, W., Huang, Y., 2022. Attenuation of antimony in groundwater from the Xikuangshan antimony mine, China: Evidence from sulfur and molybdenum isotope study. Applied Geochemistry 146, 105429. https://doi.org/10.1016/j.apgeochem.2022.105429.

Wen, B., Zhou, J., Tang, P., Jia, X., Zhou, W., Huang, J., 2023. Antimony (Sb) isotopic signature in water systems from the world's largest Sb mine, central China: Novel insights to trace Sb source and mobilization. J. Hazard. Mater. 446, 130622 https://doi.org/10.1016/j.jhazmat.2022.130622.

Wen, B., Zhou, J., Zhou, A., Liu, C., Xie, L., 2016. Sources, migration and transformation of antimony contamination in the water environment of Xikuangshan, China: Evidence from geochemical and stable isotope (S, Sr) signatures. Science of the Total Environment 569-570, 114–122. https://doi.org/10.1016/j.scitotenv.2016.05.124.

Wen, B., Zhou, J.W., Zhou, A.G., Liu, C.F., Li, L.G., 2018. A review of antimony (Sb) isotopes analytical methods and application in environmental systems. Int. Biodeterior. Biodegrad. 128, 109–116. https://doi.org/10.1016/j.ibiod.2017.01.008.

Xi, J.H., He, M.C., Wang, P.F., 2013. Adsorption of antimony on sediments from typical water systems in China: A comparison of Sb(III) and Sb(V) pattern. Soil Sed. Contam. Int. J. 23, 37–48. https://doi.org/10.1080/15320383.2013.774319.

Xia, Y., Gao, T., Liu, Y., Wang, Z., Liu, C., Wu, Q., Qi, M., Lv, Y., Li, F., 2020. Zinc isotope revealing zinc's sources and transport processes in karst region. Science of the Total Environment 724, 138191. https://doi.org/10.1016/j.scitotenv.2020.138191.

Yin, R., Feng, X., Wang, J., Li, P., Liu, J., Zhang, Y., Chen, J., Zheng, L., Hu, T., 2013. Mercury speciation and mercury isotope fractionation during ore roasting process and their implication to source identification of downstream sediment in the Wanshan mercury mining area, SW China. Chemical Geology 336, 72–79. https://doi.org/10.1016/j.chemgeo.2012.04.030.

Zhai, D., Mathur, R., Liu, S.A., Liu, J., Godfrey, L., Wang, K., Xu, J., Vervoort, J., 2021. Antimony isotope fractionation in hydrothermal systems. Geochim. Cosmochim. Acta 306, 84–97. https://doi.org/10.1016/j.gca.2021.05.031.

Zhang, C., Sun, G., Li, X., Wu, Y., Yao, H., Huang, J.H., Feng, X., 2022. Sampling and determination of antimony isotopes in airborne particles: an assessment of membrane filter materials. J. Anal. Atom. Spectrom. 37, 2713–2720. https://doi.org/10.1039/d2ja00242f.

Zhang, Z.X., Lu, Y., Li, H.P., Tu, Y., Liu, B.Y., Yang, Z.G., 2018. Assessment of heavy metal contamination, distribution and source identification in the sediments from the Zijiang River, China. Science of the Total Environment 645, 235–243. https://doi.org/10.1016/j.scitotenv.2018.07.026.

Zhong, Q., Yin, M., Zhang, Q., Beiyuan, J., Liu, J., Yang, X., Wang, J., Wang, L., Jiang, Y., Xiao, T., Zhang, Z., 2021. Cadmium isotopic fractionation in lead-zinc smelting process and signatures in fluvial sediments. J. Hazard. Mater. 411, 125015 https://doi.org/10.1016/j.jhazmat.2020.125015.

Zhou, W., Zhou, J., Feng, X., Wen, B., Zhou, A., Liu, P., Sun, G., Zhou, Z., Liu, X., 2023. Antimony Isotope Fractionation Revealed from EXAFS during Adsorption on Fe (Oxyhydr)oxides. Environ. Sci. Technol. 57, 9353–9361. https://doi.org/10.1021/acs.est.3c01906.

Zhou, W.Q., Zhou, A.G., Wen, B., Liu, P., Zhu, Z.L., Finfrock, Z., Zhou, J.W., 2022. Antimony isotope fractionation during adsorption on aluminum oxides. J. Hazard. Mater. 429, 128317 https://doi.org/10.1016/j.jhazmat.2022.128317.